SPi | Journal Code: W R C R | Article ID: 2 3 4 9 9 | Dispatch: 09.08.18 | CE: JAR | No. of Pages: 16 | ME:

AGU100 ADVANCING EARTH AND SPACE SCIENCE

Water Resources Research

RESEARCH ARTICLE
10.1029/2018WR022704

Key Points:
- Irrigation ET rates in the Central Valley increased between 1979 and 2000
- Irrigation ET rates started to decline after about 2000 as aridity continued to grow
- The irrigation ET to precipitation ratio has steadily increased over the entire study period

Correspondence to:
J. Szilagyi,
jszilagyi1@unl.edu

Citation:
Szilagyi, J., & Jozsa, J. (2018). Evapotranspiration trends (1979–2015) in the Central Valley of California, USA: Contrasting tendencies during 1981–2007. *Water Resources Research*, *54*. https://doi.org/10.1029/2018WR022704

Received 2 FEB 2018
Accepted 22 JUL 2018
Accepted article online 2 AUG 2018

Evapotranspiration Trends (1979–2015) in the Central Valley of California, USA: Contrasting Tendencies During 1981–2007

Jozsef Szilagyi[1,2] and Janos Jozsa[1,3]

[1]Department of Hydraulic and Water Resources Engineering, Budapest University of Technology and Economics, Budapest, Hungary, [2]Conservation and Survey Division, School of Natural Resources, University of Nebraska–Lincoln, Lincoln, NE, USA, [3]MTA-BME Water Management Research Group, Budapest University of Technology and Economics, Budapest, Hungary

Abstract Trends in monthly evapotranspiration (ET) rates across three watersheds covering the Central Valley in California were calculated by the latest calibration-free version of the complementary relationship of evaporation for 1979–2015. While a recent study concluded that ET rates of the irrigated fields in the Central Valley were declining in 1981–2007, here an ET trend of about 2.6 ± 12 mm per decade was found over the same period in spite of a drop in precipitation (−22 ± 30 mm per decade) and ET rates (−9.5 ± 10 mm per decade) for the rest of the watersheds, none of them statistically significant. After 2007, the precipitation decline accelerated causing a sharp drop in both irrigated and nonirrigated ET rates across the watersheds. Observations from the California Irrigation Management Information System support the present findings: Under increasing air temperatures, both dew point temperature and relative humidity values increased (at a statistically significant rate) during 1983–2007, while they reversed afterwards, in agreement with the estimated sharp irrigation ET trend decline for the remainder of the study period. Actual (in this case over irrigated fields) and reference ET rates complement each other, that is, they express opposite tendencies, as was demonstrated with California Irrigation Management Information System data, yielding a statistically significant plot-scale irrigation ET rate increase of 31 to 41 (±17) millimeters per decade for 1983–2007 in accordance with a similar drop in reference ET rates of −28 to −50 (±16) millimeters per decade, depending on whether published monthly or daily values (aggregated to monthly ones after leaving out spurious measurements) were employed.

1. Introduction

Crop irrigation in California takes place on a grand scale: Most of its vast Central Valley is covered by irrigated land (Figure 1). As often quoted, irrigation accounts for 80% of the state's water use and generates 2% of the economic output, which is not a trifle figure for a $2 trillion economy. Even an irrigation-based agricultural sector is very sensitive to weather anomalies. The last mega-drought of 2012–1015 in California cost farmers at least $2.2 billion through lost crops and increased water prices, and also eliminated, at a minimum, 17,000 jobs from the sector (Guo, 2015). The future does not look bright either in the light of the "wet regions get wetter and dry regions get drier" climate modeling wisdom (Held & Soden, 2006) that seems to hold, meaning that droughts are expected to become more frequent in the coming decades in California (Berg & Hall, 2015; Diffenbaugh et al., 2015; Yoon et al., 2015).

Irrigation at such a massive spatial scale modifies the climate and hydrology of its environment (Adoegoke et al., 2003; Christy et al., 2006; Huang & Ullrich, 2016; Jin & Miller, 2011; Kanamaru & Kanamitsu, 2008; Kueppers et al., 2007, 2008; Kueppers & Snyder, 2012; Lobell et al., 2009; Lobell & Bonfils, 2008; Ozdogan et al., 2010; Sacks et al., 2009; Sorooshian et al., 2011, 2012, 2014; Szilagyi, 2018a; Yang et al., 2017). For example, Lobell and Bonfils (2008) observed a 2.5–3 °C mean daily summertime air temperature difference between extensive irrigated and nonirrigated land areas in the Central Valley. Some of the changes may occur at a regional scale too, reaching as far as the Great Basin (Wei et al., 2013) and the Colorado River watershed (Lo & Famiglietti, 2013) in the form of irrigation-boosted precipitation and the resulting increased streamflow, just to name the most obvious hydrological variables.

For studying how irrigation has changed and reformed the climate and hydrology of the region both global and regional climate models (GCM and RCM, respectively) have been employed in the past (see Mahmood et al., 2010, and Pielke Sr et al., 2011, for a review). More recently, Sorooshian et al. (2014) investigated the

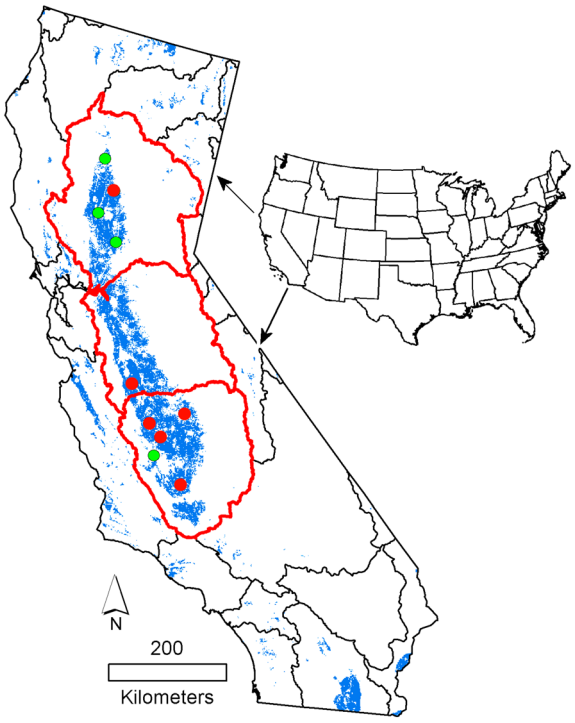

Figure 1. Location of the hydrologic unit code six-level watersheds (outlined in red) covering the Central Valley in California. The blue dots represent 1-km^2 grid cells (Brown & Pervez, 2014) with more than 50% irrigated field cover. The green (monthly data only) and red (daily and monthly data) dots denote the location of those California Irrigation Management Information System stations that provided data for the present study.

influence of irrigation in the Central Valley to hydrological processes of the broader region. Employing the National Centers for Environmental Prediction (NCEP) reanalysis-I data in the National Center for Atmospheric Research NCAR/PENN STATE mesoscale model (MM5), as well as utilizing in situ observations of the California Irrigation Management Information System (CIMIS), they concluded that irrigated land evapotranspiration (ET) rates had decreased over the 1981–2007 time period. Their conclusion was based on declining ET rates coming from a modified (to account for irrigation) MM5 model and similarly declining CIMIS reference ET rate (E_o) values, and attributed these declines to dropping trends in MM5-obtained shortwave and longwave downwelling radiation, and 2-m air temperature. CIMIS employs the Penman-Monteith equation of Allen et al. (1998) as well as a modified Penman (1948) equation (similar to the one below) for the E_o calculations. See the CIMIS site (http://www.cimis.water.ca.gov) for more information.

In this study, aided by North American Regional Reanalysis (NARR; Mesinger et al., 2006) and Parameter Regressions on Independent Slopes Model (PRISM) data (Daly et al., 1994) as well as by CIMIS measurements, it is argued and provided support for that such a decline in irrigation ET rates had not taken place over the 1981–2007 period as Sorooshian et al. (2014) concluded. By extending the study period to 2015, it is also demonstrated that a significant overall decline in irrigation ET rates (following a previous increase) had indeed started to occur after about the turn of the century across the Central Valley of California.

The complementary relationship (CR) of evaporation, first introduced by Bouchet (1963), has progressed significantly in recent years. It is the only ET estimation approach that does not require any information on land surface properties, such as land use/land cover or soil moisture content (the latter typically requiring some water budgeting), types of data climate or their land surface model (LSM) components typically ask for. The CR (Brutsaert, 2015; Brutsaert & Stricker, 1979; Crago et al., 2016; Huntington et al., 2011; Morton, 1983; Szilagyi, 2015; Szilagyi, 2018b; Szilagyi et al., 2017) recognizes that over a certain time interval—typically a day or longer—and on a regional scale (typically in excess of a kilometer), the lower atmosphere will fully adjust itself to the moisture status of the underlying (homogeneous) land surface. Note that the land surface can behave homogeneously at the regional scale if the typical scale of the inhomogeneity is much smaller than the regional extent and/or when the large-scale gradient of any surface property is minor. It has also been found that the typical spatial extent over which the lower atmosphere will adjust itself across jumps in surface property is again on the order of a kilometer (de Vries, 1959; Dyer & Crawford, 1965; Rao et al., 1974; Rider et al., 1963). The chosen ~4-km resolution of the PRISM data set therefore is ideally suited for a regional-scale application of the CR approach.

A comprehensive study by McMahon et al. (2013a, 2013b) found the CR approach as the most reliable actual ET estimation method that uses standard atmospheric variables. Also, Szilagyi (2018b) in a U.S.-wide study demonstrated that the CR version explained below and employed with regional-scale data significantly outperforms the ET rate values of NCEP, provided with the NARR data.

Both versions of the CR—that is, that of Morton et al. (1985), employed with the plot-scale CIMIS data and the one by Szilagyi et al. (2017) applied on the regional scale—in the present study have the added advantage that they are calibration free and universally applicable. In fact, the ~4-km resolution monthly ET rates in the present study come—without any modifications—from the work of Szilagyi (2018b) who obtained them for the entire coterminous United States over the 1979–2015 period. The calibration-free nature of the present CR approach avoids the type of (often guess work) modifications Sorooshian et al. (2014) needed to perform on their RCM of choice to account for the effect of irrigation. In fact, it is argued here that the CR approach, vastly overlooked by the hydrometeorology/climate modeling community, could benefit any RCM or GCM applications/developments by providing latent heat fluxes the LSM-estimated flux values

could be validated with and calibrated against (and thus the LSMs improved), which so far has not happened to the best knowledge of the present authors.

2. Description of Methods and Data

The CR method derives the actual ET rate by comparing how the evaporation rate (E_p) of a small wet surface, boosted by horizontal energy advection (Brutsaert, 1982) from the drying land, differs from that (E_w) of a regional-scale wet surface, let us say after a regional-extent heavy downpour when both the surface radiation balance (R_n) and wind conditions have more-or-less resumed to prestorm conditions. This does not mean that wet environment air temperature (T_w) would be the same as before the storm (i.e., T_a) since the wet surface evaporation exerts a significant cooling effect on the land and in the air in contact with it. The CR correctly observes that the larger the difference between E_p and E_w the smaller actual ET is, or as Brutsaert and Stricker (1979) formulated it in their advection-aridity (AA) model

$$E_p - E_w = E_w - ET \tag{1}$$

where E_p is estimated by the Penman (1948) equation

$$E_p = \frac{\Delta(T_a)}{\Delta(T_a)+\gamma} R_n + \frac{\gamma}{\Delta(T_a)+\gamma} f_u[e^*(T_a) - e^*(T_d)] \tag{2}$$

Here T_d is the dew point temperature, Δ the slope of the saturation vapor pressure curve at T_a, γ is the psychrometric constant, e^* the saturation vapor pressure, and f_u (mm d^{-1} hPa^{-1}) the wind function, traditionally formulated as 0.26 (1 + 0.54u_2), where u_2 is the horizontal wind speed (m/s) 2 m above the ground. R_n is expressed in water equivalents (mm/day). Note that $e^*(T_d) = e_a$ is the actual vapor pressure, while $e^*(T_a) - e_a$ and $e_a/e^*(T_a)$ are called the vapor pressure deficit (*VPD*) and relative humidity (*RH*), respectively. The wet-environment ET rate is specified by the Priestley and Taylor (1972) equation

$$E_w = \alpha \frac{\Delta(T_w)}{\Delta(T_w)+\gamma} R_n \tag{3}$$

where α is the Priestley-Taylor coefficient, having an empirical value between 1.1 and 1.3. In typical applications α is taken as a calibration coefficient, allowing for replacing the unknown T_w by the measured T_a. Szilagyi et al. (2017) described a model-independent method of estimating α, obtaining a value of 1.15, employed in Szilagyi (2018b).

In order to avoid the typical calibration of α and the application of the frequently missing wind speed value, Morton (1983) introduced a vapor transfer coefficient that depends on air stability only which he derived from R_n (estimated from solar radiation, R_s), and the humidity of the air. The resulting computer program, called WREVAP (Morton et al., 1985), to be employed with CIMIS data because it estimates R_n directly from the CIMIS-measured R_s (in Langley per day), keeps the symmetric nature of ((1)).

In the past decades, evidence mounted that a symmetric CR (without proper accounting for the surface temperature change between drying and wet conditions, thus making the $E_p - E_w$ difference smaller in ((1)) and so ET closer to E_w) overestimates actual ET rates in arid environments (Hobbins et al., 2001; Huntington et al., 2011; Szilagyi & Jozsa, 2008). Note that this is not a hindrance as WREVAP is to be applied over irrigated fields that together yield a regional extent in this study, where the resulting ET rates are much larger (while surface temperatures are much colder) than would come from a nonirrigated arid area. It should be noted here also that in the Hobbins et al. (2001) paper the wind speed values were measured at 10 m above the ground and were not transferred to 2 m height (personal communications) as required by ((2)). That is the main reason that on a U.S.-wide basis their AA model underestimated water-balance ET by more than 10% of the corresponding precipitation value and that the typical overestimation of their AA model in arid environments was not apparent in their work (while that of WREVAP was), but it is obvious in Szilagyi and Jozsa (2008).

To account for the varying degree of asymmetry (Szilagyi, 2007) typically found in the CR applications, Brutsaert (2015) introduced a nonlinear formulation

$$y = (2 - X)X^2 \tag{4}$$

with the scaled variables $y = ET/E_p$, and $X = E_w/E_p$. Crago et al. (2016) and Szilagyi et al. (2017) further improved the scaled variable X to $X = (E_{pmax} - E_p)\,(E_{pmax} - E_w)^{-1}\,E_w/E_p$ by realizing that E_w/E_p is limited by the maximum possible value of E_p (E_{pmax}) so that the ratio cannot in general approach zero, unless E_w itself does so. Szilagyi et al. (2017) defined E_{pmax} with the help of ((2)) by applying it to a superarid environment of air temperature T_{dry} and where actual vapor pressure is negligible

$$E_{p\max} = \frac{\Delta(T_{dry})}{\Delta(T_{dry}) + \gamma} R_n + \frac{\gamma}{\Delta(T_{dry}) + \gamma} f_u e^*(T_{dry}) \tag{5}$$

T_{dry} is the dry-environment air temperature the moist air would assume during adiabatic drying of the surface (Szilagyi et al., 2017)

$$T_{dry} = T_{wb} + \frac{e^*(T_{wb})}{\gamma} \tag{6}$$

where T_{wb} is the wet-bulb temperature. T_{wb} can be obtained from the (quasi) adiabatic process (Monteith, 1981; Szilagyi, 2014) occurring at the wet-bulb thermometer, yielding an implicit equation

$$\gamma \frac{T_{wb} - T_a}{e^*(T_{wb}) - e^*(T_d)} = -1 \tag{7}$$

similar to the one (see below) employed by Szilagyi (2014) for deriving T_w in ((3)). As this latter temperature is not known under typically drying conditions, it can be approximated by the wet-environment surface temperature, T_{ws} (under humid conditions the vertical air temperature gradient is relatively small in comparison with drying conditions; Szilagyi & Jozsa, 2009), as long as it is smaller than T_a; otherwise, T_w in ((3)) can be replaced by T_a since in reality $T_w \leq T_a$ due to the cooling effect of evaporation (Szilagyi, 2014). T_{ws}, however, can be obtained implicitly (Szilagyi, 2014) from the Bowen ratio, B_o, of the small wet patch ((2)) is applied for, that is,

$$B_o = \frac{H}{LE} \approx \frac{R_n - E_p}{E_p} \approx \gamma \frac{T_{ws} - T_a}{e^*(T_{ws}) - e^*(T_d)} \tag{8}$$

where H is sensible and LE the latent heat flux (i.e., E_p in energy-flux units) at the small, wet surface.

Equations ((2))–((8)) were employed across the coterminous United States at a monthly time step over the 1979–2015 period (Szilagyi, 2018b) employing 32-km resolution NARR R_n (prepared from upwelling and downwelling shortwave and longwave radiation flux components) and 10-m wind, u_{10}, data downloaded from esrl.noaa.gov/psd/data/gridded/data.narr.html. The u_{10} values were turned into 2-m horizontal wind velocities via a power transformation of $u_2 = u_{10}(2/10)^{1/7}$ (Brutsaert, 1982). The NARR values were then linearly interpolated over the ~4-km grid of the PRISM T_a, T_d, and precipitation (P) values (the last one for validation only), available from prism.oregonstate.edu. PRISM data are one of the most thoroughly validated land-based data set for the conterminous United States (Daly et al., 2008).

Equations ((2))–((8)) resulted in monthly cell ET rates that were aggregated into annual values and then spatially averaged for each year over the study area to be validated as the difference in similarly aggregated and averaged PRISM P and U.S. Geological Survey's six-level hydrologic unit code (HUC6, Figure 1) streamflow (Q) rates (from waterwatch.usgs.gov). The upper watershed in Figure 1 is called the Lower Sacramento (Seaber et al., 1987) with a drainage area (D_a) of 51,541 km^2, the middle one the San Joaquin (D_a = 40,404 km^2), and the lower one the Tulare-Buena Vista Lakes catchment (D_a = 41,959 km^2). A similar validation was performed for the linear trend of the study-area averaged annual ET rates.

Here, as a working hypothesis for a water-balance-based validation of the ET rates, is assumed that changes in groundwater and soil moisture (ΔS) between the end and start of the 27 (1981–2007) and 37 (1979–2015) years of the model periods are negligible in comparison with the time period integrated incoming (P) and outgoing (Q) flux values. Below it is shown that this assumption is acceptable even in the face of the general groundwater decline evidenced by the GRACE data (Tapley et al., 2004) for the 2002–2015 period. The long-

Table 1
List of CIMIS Stations Employed in the Study (Figure 1)

Station name	Latitude (°)	Longitude (°)	Elevation (m)	Record start	Record end
Five Points[a]	36.336	−120.112	95	6/7/1982	Active
Shafter[a]	35.532	−119.281	120	6/1/1982	Active
Firebaugh[a]	36.851	−120.59	62	9/22/1982	Active
Gerber	40.044	−122.165	84	9/22/1982	8/14/2014
Durham[a]	39.608	−121.824	43	10/19/1982	Active
Stratford[a]	36.158	−119.851	65	10/29/1982	Active
Kettleman	35.867	−119.894	114	11/19/1982	9/1/2017
Nicolaus	38.87	−121.546	11	1/3/1983	12/29/2011
Colusa	39.226	−122.024	18	1/13/1983	8/12/2016
Parlier[a]	36.597	−119.504	113	5/23/1983	Active

[a]Stations that publish daily values on top of monthly ones.

term mean annual ET rate estimation as the difference in similar P and Q values further assumes that interbasin water transfers are also negligible (some corrections will be applied below) and that the net lateral groundwater flux is zero for the study area.

For the evaluation of regional-scale irrigation ET rates the 1-km resolution MIrAD land-irrigation (Brown & Pervez, 2014) data set was used. It specifies the percentage of irrigated land in each 1-km^2 cell for the entire coterminous United States.

The WREVAP FORTRAN code of Morton et al. (1985; downloadable from snr.unl.edu/szilagyi/szilagyi.htm) was also applied with monthly data (T_a, e_a, and R_s from cimis.water.ca.gov) coming from 10 different CIMIS stations (Figure 1) across the Central Valley to validate the ET trend estimates of ((2))–((8)) for irrigated areas with input data obtained independently from the NARR and PRISM values. For a list of station names and locations, see Table 1. Stations with the longest available record were selected from locations of abundant irrigation around the station, mentioned in the location description file. Any missing monthly value in the CIMIS data was substituted by its multiyear mean value of the month, separately for each station. ET calculations started in 1983, the first full year of records, similar to Sorooshian et al. (2014).

To double check the reliability of the general trends observable in the monthly CIMIS data those stations, that is, six out of the 10 already selected (Table 1 and Figure 1), that also had published daily values were reselected and their untagged daily values were aggregated to monthly ones before rerunning the WREVAP code. Any values with the "ignore" and "way out of range" tags were dropped, except for precipitation where only the "ignore" tag was considered for annulling the data, because otherwise an about 15-year long period of no precipitation would have occurred for one (i.e., Shafter) of the stations. Also, some spuriously high precipitation values without any tag for 6 years in a row for one station (i.e., Firebaugh) were similarly omitted. As wide-spread quality assurance and control problems may exist in agricultural network weather data (Allen, 1996; Allen et al., 1998; ASCE-EWRI, 2005; Huntington et al., 2015) such as provided by CIMIS, the resulting trends in them should be treated with caution and considered only as general tendencies.

It is important to point out that the CR can be applied at the plot scale of the irrigated fields because they form a more or less continuous irrigated region within the Central Valley (Figure 1), thus meeting the scale requirement explained in the Introduction. Note that the CR takes into consideration the possibility that an irrigated field may not evaporate at the potential rate due to reasons discussed later. The CIMIS reference ET approach however assumes that the reference vegetation cover, that is, actively growing mowed grass, does evaporate at the potential ET rate of E_o. (It must be mentioned that the E_o value cannot directly tell one at what rate other irrigated crops evaporate, only after an application of a crop-specific coefficient that depends also on the stage of development of the crop itself.) This is a fundamental difference because under a constant R_n term but dropping VPD values (see (2)), E_o would be declining and thus implying a general drop in irrigation ET rates of all crops (as Sorooshian et al., 2014, assumed), while the former a growing one, since in the CR the VPD drop is caused by more intensive (in this case) irrigation ET rates at a regional scale, as the region is a mosaic of such irrigated fields (Figure 1).

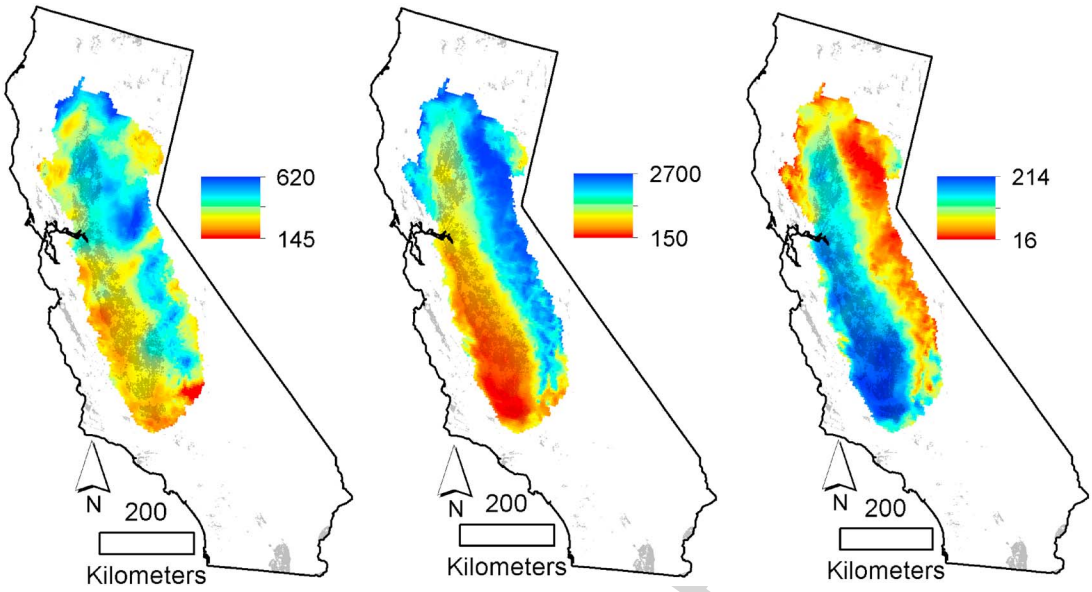

Figure 2. Mean (1979–2015) annual (a) ET (mm), (b) precipitation (mm), and (c) ET_r (%) distributions across the study area. The gray dots represent MIrAD cells with more than 50% irrigated-land cover. The spatial averages with the corresponding standard deviation values are as follows: ‹ET› = 387 ± 74 mm; ‹*P*› = 700 ± 445 mm; and ‹ET_r› = 78 ± 43%, respectively. The maximum and minimum values are displayed in the legend.

3. Results and Discussion

3.1. Regional-Scale ET Rates and Their Trends

Figure 2 displays the CR-derived (i.e., equations ((2))–((8))) mean annual ET, *P*, and ET ratio (i.e., ET_r = ET/*P*) dis- F2
tributions. Note that the highest ET and precipitation rates are typically found in high altitudes (Sierra Nevada and Klamath mountain ranges) where the ET ratios are the smallest due to lower temperatures, shallower soils, and a steeper terrain than what is found in the valley. Due to large-scale irrigation the ET ratios rise above 100% in the Central Valley, as more water is evaporated from the irrigated land than what it receives in the form of precipitation, especially in the San Joaquin Valley where precipitation is the scarcest.

While the spatial average, ‹ET_i› = 369 ± 62 mm, of the mean annual irrigation ET value (over MIrAD cells with a value larger than 50%) is somewhat lower than that of no-irrigation land ET (i.e., cells with MIrAD value of zero), that is, ‹ET_{noi}› = 392 ± 77 mm, there is a large difference in both irrigation and no-irrigation *P* and ET_r values: ‹P_i› = 330 ± 133 mm versus ‹P_{noi}› = 830 ± 450 mm and ‹ET_{ri}› = 124 ± 34% versus ‹ET_{rnoi}› = 63 ± 35%, respectively. Note that the spatial average of the ET ratios, ‹ET P^{-1}›, is different from ‹E›‹*P*›$^{-1}$. The latter has a value of 112% for irrigated land, 47% for no-irrigation areas, and 55% for the study area as a whole. By restricting the time period to 1981–2007 (which thus excludes the drought of 2012–2015), the spatially averaged mean annual irrigation ET rate becomes ‹ET_i› = 382 ± 62 mm, which is practically identical to the 386-mm irrigation ET rate of the original version of MM5, reported by Sorooshian et al. (2014).

For a validation of the study area averaged mean annual ET rate of 387 mm (Figure 2), the mean annual HUC6 discharge rates were area-averaged to result in ‹*Q*› = 231 mm, which when subtracted from the 700 mm ‹*P*› value yields 469 mm, about 20% larger than the CR-derived ET value. If one employs a fairly stable annual municipal water use estimate of about 10% of the mean annual streamflow, typical in California (see Figures 3–10 of State of California, 2013; Figure 2.4 and Table 2.2 of Hanak et al., 2011; as well as Mount & Hanak, 2016) and further assumes that this figure is valid for the study area, as well as considers that municipal water is carried in large capacity pipes and canals from reservoirs in the mountains to the urban areas then this water, unaccounted for in the HUC6 discharge values, must be added to the mean annual discharge rate which thus increases to ‹*Q*› = 257 mm. This way the CR ET value of 387 mm/year is within 13% of the water-balance value of 443 mm/year. As Hanak et al. (2011) note, any water use estimate in California is "hampered by a lack of local reporting," so the 10% municipal water use value for the study area is possibly fraught with an unquantified large error.

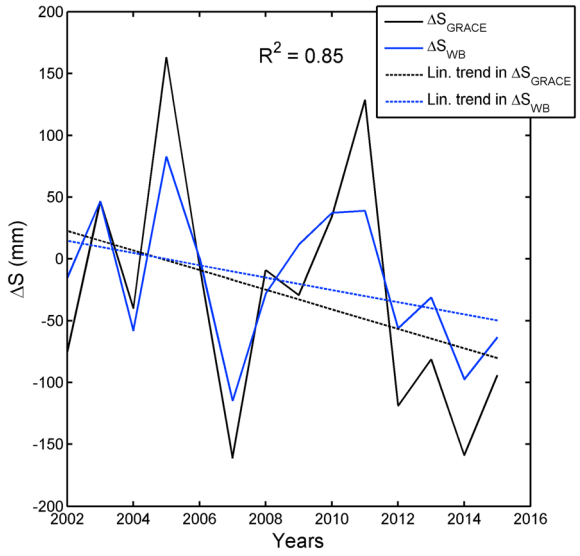

Figure 3. GRACE and water-balance (WB)-derived annual changes (for water years) in water storage (ΔS) within the study area of Figure 1 during 2002–2015.

The modeled annual ET rates of the study area were further tested by annual changes in the GRACE-derived terrestrial water storage (S_{GRACE}) values (Tapley et al., 2004) over the available 2002–2015 time period. The water-balance derived annual (written for water years) storage changes (ΔS_{WB})

$$\Delta S_{WB} = P - Q - ET \tag{9}$$

(where the Q values include the assumed constant 25.7-mm annual municipal water use figure) were compared to similar changes (ΔS_{GRACE}) in the S_{GRACE} values obtained by NASA's Jet Propulsion Laboratory, downloadable from http://ccar.colorado.edu/grace/jpl.html. For the annual changes the original S_{GRACE} values, available for certain days of the year, were interpolated by a spline method to yield a value for each day of the 2002–2015 period. The annual changes, ΔS_{GRACE}, then result by taking the difference in the S_{GRACE} values for 1 October in each consecutive years. For the 2002 water year the first available published value was used in lieu of the 1 October value of the previous year. Application of water years (in place of calendar years) in ((9)) for the storage change was prompted by the Mediterranean-like climate of California with winter precipitation maxima, thus making the January storage values dependent on actual rain events. For the annual sums of the P, Q, and ET values this choice of calendar versus water year is less important, therefore the use of calendar years in the rest of the study.

The ΔS_{WB} values of Figure 3 explain 85% of the variance expressed by the ΔS_{GRACE} values, a strong indication F3 that the CR-derived ET values are quite reliable, at least, on an annual basis. The observed linear trend values in the two time series are −79 ± 61 mm per decade for GRACE, and −49 ± 36 mm per decade for the water-balance values. Neither trend is statistically significant. Note that the GRACE-recorded annual storage decline of −7.9 mm/year (even when assumed valid for the entire modeling period of 1979–2015) is only 2% of the estimated mean annual ET rate of 387 mm/year, well within the 74 mm/year standard deviation value.

Figure 4 displays linear tendencies in the CR-derived ET rates for 1979–2015 and 1981–2007. As the full study F4 period includes the serious drought years of 2012–2015, it is not surprising that the ET trend decline is stronger (and statistically significant at the 5% level) than in the period preceding the drought, especially that precipitation behaved similarly (Figure 5). But there is also an important difference in the spatial distribution of F5 the trend values between the two periods even though precipitation and thus ET rates in both periods declined the strongest in the mountains. While for 1979–2015 ET rates were dropping over the entire study area, in 1981–2007 ET rates dropped only in the mountains but they were generally increasing (or at least stayed about constant) within the valley despite of declining precipitation there too (Table 2). T2

Validation of the linear tendencies in regional ET rates can be performed with the help of similar, area-averaged, tendencies in streamflow rates that amount to −42 and −33 mm per decade for the two periods, 1979–2015 and 1981–2007, respectively. Here no spatial variance is calculated because sample size is only three. When the two ET trends of Figure 4 are added to these values they yield −62 and −39 mm per decade, which are within 8% and 4% of the trends observable in the precipitation values, that is, −58 and −38 mm per decade in Figure 5, a remarkable accuracy.

Long-term tendencies of ET and precipitation rates over irrigated and nonirrigated land are displayed in Figure 6. A polynomial trend approach was preferred for the longer time period in order to see how the trend F6 changed, if at all, with time. The applied third-order polynomial equations have the required flexibility for time dependent trend-changes that may even swap sign yet are the least influenced by any single year's value. A PRISM cell is considered irrigated if more than 50% of its area is irrigated land according to MIrAD data. While precipitation expresses an overall declining trend in both time periods (1979–2015 and 1981–2007), irrigation ET and the irrigation ET ratio increase between 1981 and 2007 (not to a statistically significant degree) under a continuously warming climate (Figure 7). This is possible because the farmers will most likely F7 supplement the missing precipitation with irrigation water up to a point, that is, when it becomes too expensive due to increased demand. Then leaving the land to go fallow or selling the water rights to, for example,

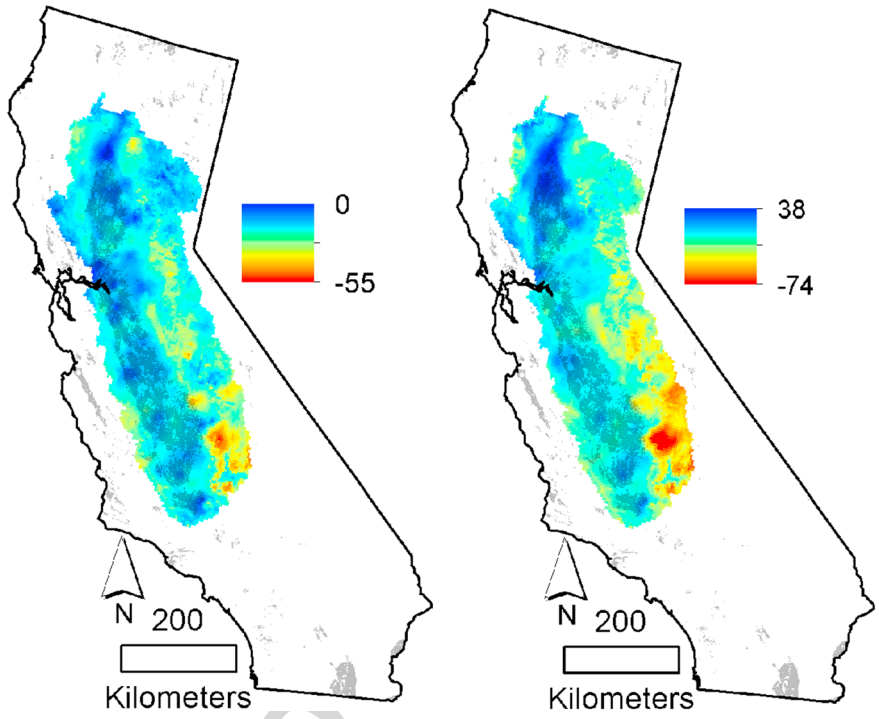

Figure 4. Linear trend values (mm per decade) in the complementary relationship-derived mean annual ET rates for (a) 1979–2015 and (b) 1981–2007. The spatial averages with the corresponding standard deviation values are as follow: $-21 \pm 7^{*}$ and -6.3 ± 14 mm per decade, respectively. The maximum and minimum values are displayed in the legend. *The trend is significant at the 5% level.

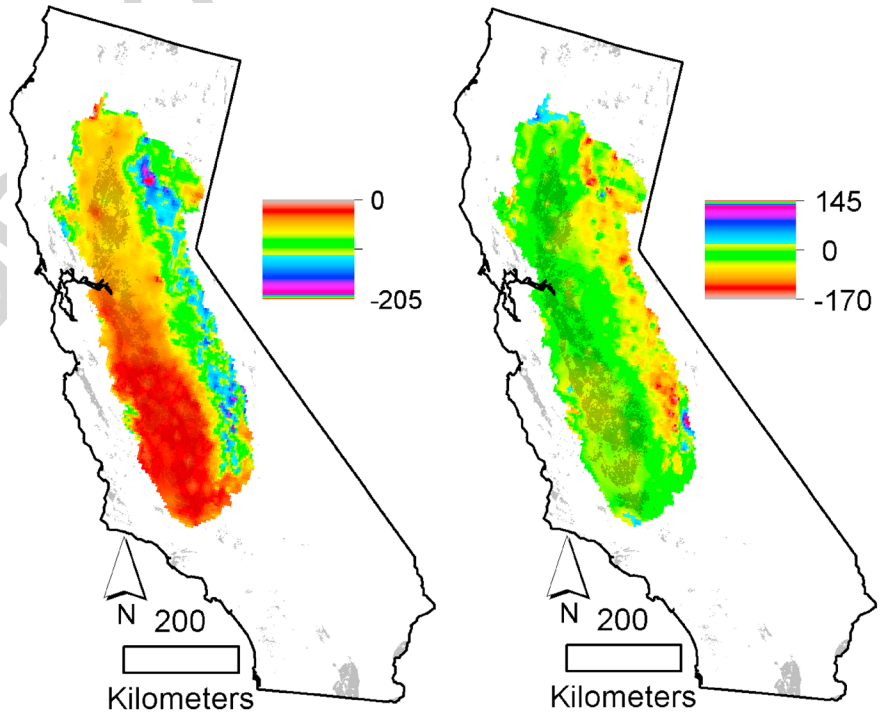

Figure 5. Linear trend values (mm per decade) in precipitation rates for (a) 1979–2015 and (b) 1981–2007. The spatial averages with the corresponding standard deviation values are as follows: -58 ± 35 and -38 ± 28 mm per decade, respectively. The maximum and minimum values are displayed in the legend.

Table 2
Linear Trend Statistics (1981–2007) of the Regional-Scale Annual Time Series

Trend variable	Trend value	Standard deviation	Mann-Kendall p value (–)
ET, irrigated (mm per decade)	2.6	12	0.77
ET, nonirrigated (mm per decade)	−9.5	10	0.4
P, irrigated (mm per decade)	−22	30	0.8
P, nonirrigated (mm per decade)	−43	70	0.83
ET_r, irrigated (decade^{-1})	0.04	0.07	0.67
ET_r, nonirrigated (decade^{-1})	−0.005	0.03	0.59
T_a, irrigated (°C per decade)	0.17	0.11	0.26
T_a, nonirrigated (°C per decade)	0.4	0.12	0.003**
T_d, irrigated (°C per decade)	0.16	0.19	0.53
T_d, nonirrigated (°C per decade)	−0.012	0.19	0.45
VPD, irrigated (hPa per decade)	0.1	0.16	0.56
VPD, nonirrigated (hPa per decade)	0.42	0.16	0.02**
RH, irrigated (% per decade)	0.04	0.7	0.87
RH, nonirrigated (% per decade)	−1	0.79	$3.62{\cdot}10^{-4}$**
R_n, irrigated (mm per decade)	−9.2	5.9	$2{\cdot}10^{-8}$**
R_n, nonirrigated (mm per decade)	−9.4	4.7	0.06*
u_2, irrigated (m s^{-1} decade^{-1})	−0.006	0.02	0.96
u_2, nonirrigated (m s^{-1} decade^{-1})	−0.006	0.02	0.65

*Test significant at the 10% level. **Test significant at the 5% level.

municipalities (Guo, 2015), may become more lucrative to many farmers than what they could produce with that water; so irrigation, and therefore ET rates, will start to decline within the valley. That is what most likely happened after 2007, which also was a drought year but less severe than the mega-drought of 2012–2015. As seen, the irrigation ET rates did not decline as fast as precipitation rates did, since the ET ratio shot up even higher than before.

The ET ratio behaves in a complementary way to precipitation: In a dry year the ET ratio increases as more water will infiltrate the dry soil and be used by the vegetation leaving relatively less to runoff than in a wet year. The rough mountainous terrain with thinner soils, however will cut back on infiltration capacity and will boost runoff more than the flat valley bottom, that is why the ET ratio did not increase between 1981 and 2007 over nonirrigated land, but afterwards, with a drastic drop in precipitation rates, it rose even there.

Table 2 summarizes the linear trend values (and their standard deviations; Nau, 2017) of the mean annual ET rates and other meteorological variables over 1981–2007 together with the Mann-Kendall p value (Hamed & Rao, 1998) of the linear trend test. The trend is significant if the p value is less than 0.1 or 0.05, which are the two most commonly applied significance levels of 10% and 5%, respectively.

As a result of increasing irrigation ET rates in 1981–2007, the dew point temperatures and even RH increased (or at least stayed constant) in the valley while both declined (RH at a statistically significant level, see Table 2) in the mountains (Figure 7). Beginning in the years following 2000, they started to drop in both areas in an accelerating fashion with sharply falling ET rates due to failing precipitation. The T_d-rate increase in the valley however could not keep up with the air-temperature rise (this latter is statistically significant in the mountains); thus, VPD values tended to increase in both areas. A quite possible reason that air temperature in the valley did not rise as fast as in the mountains is irrigation itself: When the latter started to decline, air temperatures started to rise sharply in the valley too (Figure 7).

Interestingly, net radiation, R_n, at the surface was falling at a statistically significant rate over the entire study period in both regions while at the same time air temperature increased. The NARR solar radiation (R_s) values (not displayed) were increasing (although not at a statistically significant level) during the entire modeling period for the whole study area. Increasing R_s values (combined with weakening winds from Figure 7 and Table 2) can explain the observed slight temperature change in irrigated areas in a period when CR-estimated ET rates were also increasing during 1981–2007. A general R_s increase in the Central Valley over the modeling period is further supported by the Climate Engine (app.climateengine.org) data visualization site (Huntington et al., 2017). The dropping R_n values during 1981–2007 are then the result of increasing thermal radiation from the land surface due to insolation-driven elevated surface temperatures further boosted by failing winds.

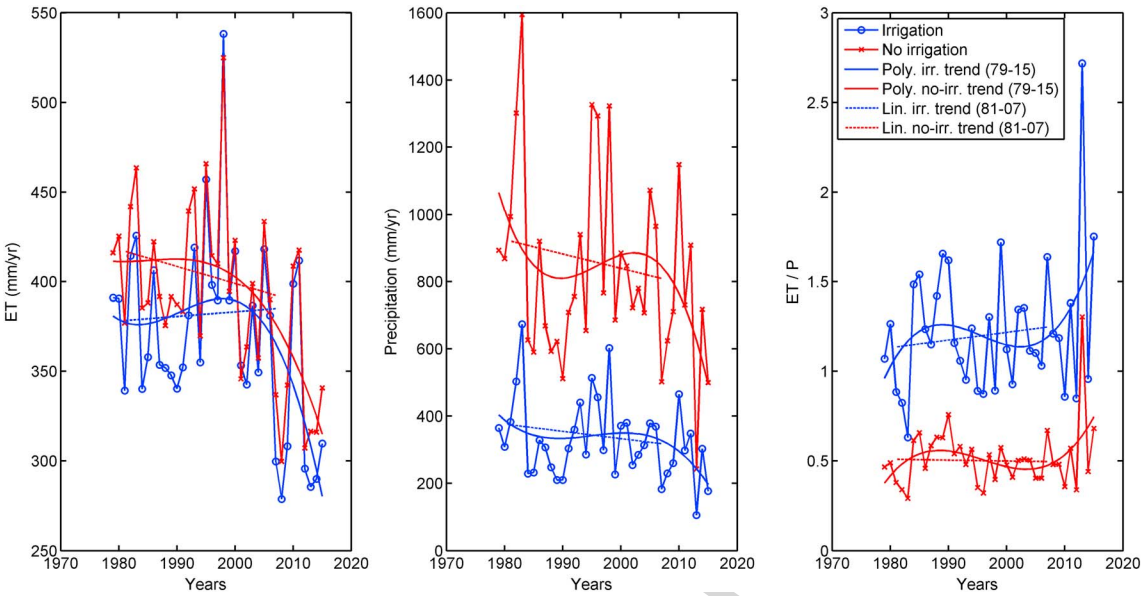

Figure 6. Annual ET, *P*, and ET-ratio values and their best-fit linear (1981–2007) and third-order polynomial (1979–2015) curves by the presence/absence of irrigation. ET = evapotranspiration.

While the declining trend in R_n may also fall in line with the declining downwelling radiation reported by Sorooshian et al. (2014), the linear tendencies found in irrigation ET rates, air temperature, and water vapor content of the air (directly related to T_d) for 1981–2007 are opposite to what Sorooshian et al. (2014) reported for the same time period. If the trend analysis is restricted to July–August only (similar to Figure 6 of Sorooshian et al., 2014), the time of most intensive irrigation in the valley, the only variable that shows a different linear trend in the annual values for 1981–2007 from those above (i.e., R_n, T_a, T_d, and irrigation ET) is R_n and that is only over nonirrigated areas. Also, annual precipitation rates of Sorooshian et al. (2014) did not display any clear tendency, while the PRISM data express declining rates overall (Figure 6), independent of the presence or absence of irrigation. The linear trend differences between the two studies may come from the differing sources of data, that is, NCEP reanalysis-I with MM5 for Sorooshian et al. (2014) and NARR (R_n and u_2) and PRISM (T_a, and T_d) for this study. This obvious discrepancy in the sought-after ET rate tendencies

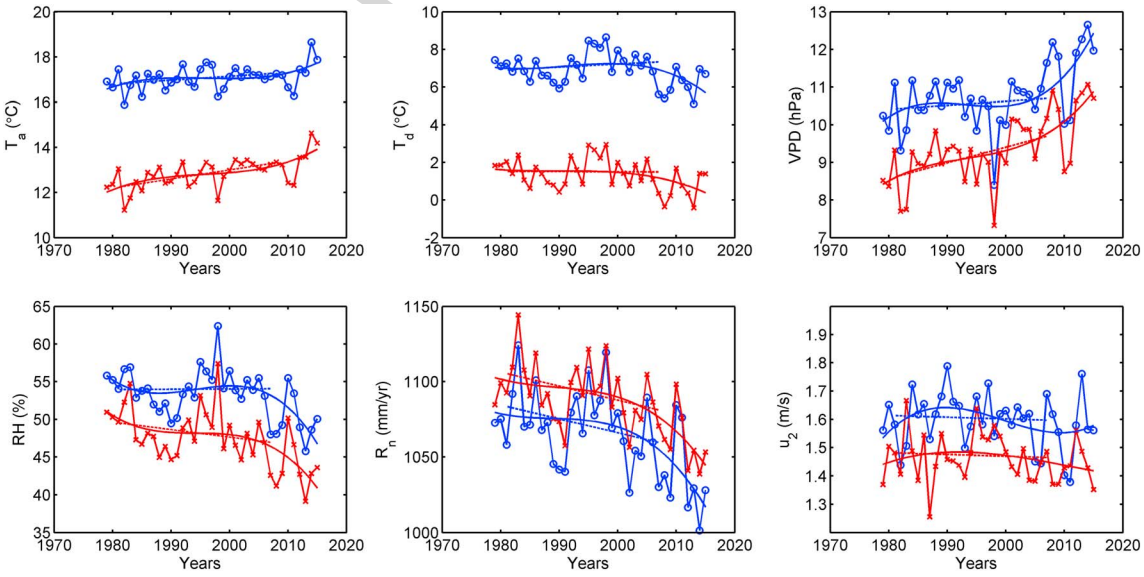

Figure 7. Annual T_a, T_d, *VPD*, *RH*, R_n, and u_2 values and their best-fit linear (1981–2007) and third-order polynomial (1979–2015) curves by the presence/absence of irrigation. For a legend, see Figure 6. RH = relative humidity; VPD = vapor pressure deficit.

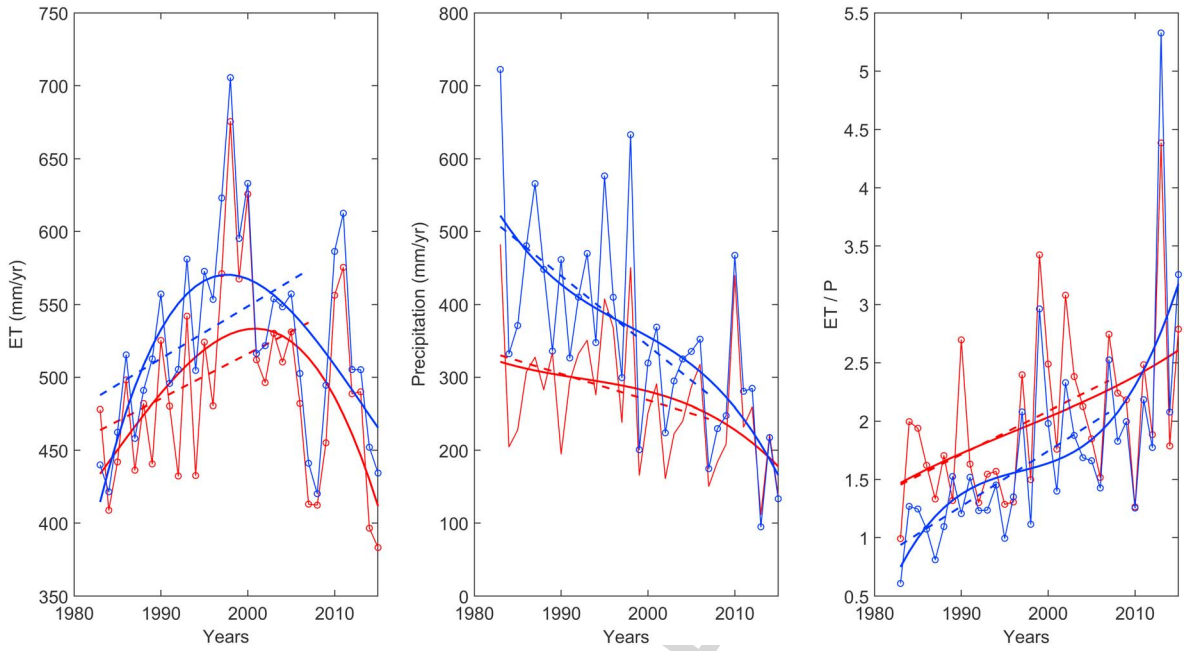

Figure 8. Station-averaged annual ET, *P*, and ET-ratio values and their best-fit linear (1983–2007) and third-order polynomial (1983–2015) curves for CIMIS stations with the longest available record (i.e., starting in 1983 or earlier) in an area of abundant irrigation. Data from published (a) monthly values of 10 stations (blue) and (b) daily values (aggregated to monthly ones) of six stations (red). ET = evapotranspiration.

however makes it necessary to validate or disprove the present results with in situ measurements of the CIMIS sites.

3.2. Plot-Scale ET Rates and Their Trends

The CIMIS stations in California are deliberately located within irrigated areas to provide information about reference ET (E_o), its atmospheric drivers, and at selected locations, about the soil moisture status. Reference ET is the estimated ET rate of a plot-sized, well-irrigated and mowed, actively growing grass. As

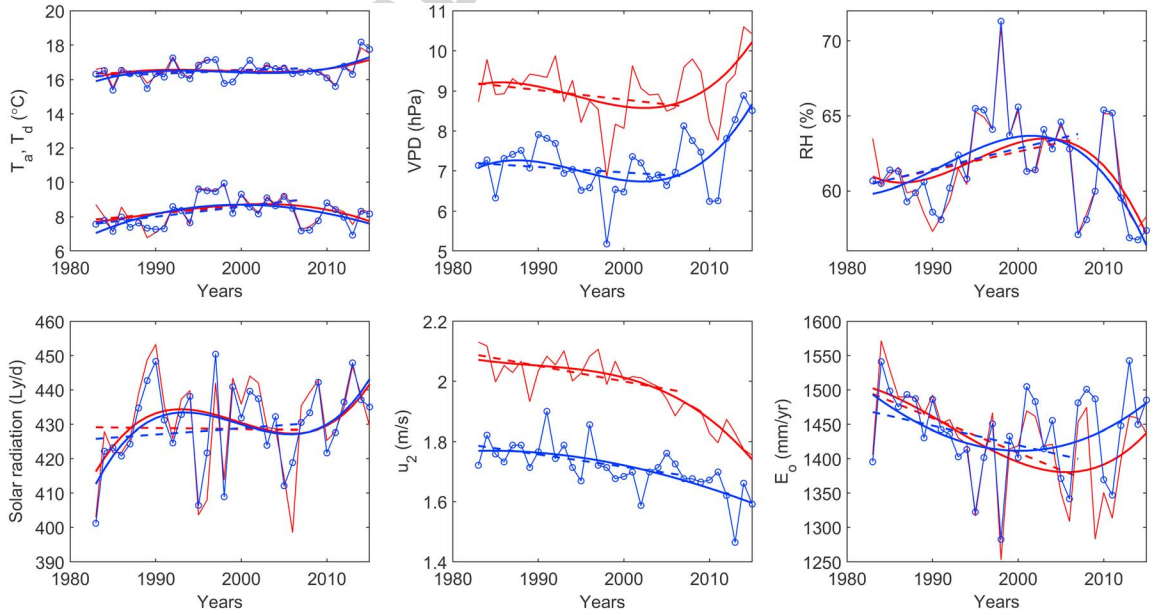

Figure 9. Station-averaged annual T_a, T_d, *VPD*, *RH*, R_s, u_2, and E_o values and their best-fit linear (1983–2007) and third-order polynomial (1983–2015) curves for the CIMIS stations in Figure 8. Data from published (a) monthly values of 10 stations (blue) and (b) daily values (aggregated to monthly ones) of six stations (red). RH = relative humidity; VPD = vapor pressure deficit.

Table 3
Linear Trend Statistics (1983–2007) of the CIMIS Station Averaged (From Monthly Values of 10 Stations and From Daily Values, Aggregated to Monthly Values, of Six Stations [in Parentheses]) Annual Time Series

Trend variable	Trend value	Standard deviation	Mann-Kendall p value (−)
ET (mm per decade)	41 (31)	17 (17)	0.01** (0.076*)
P (mm per decade)	−96 (−36)	31 (22)	0.008** (0.25)
ET_r (decade^{-1})	0.5 (0.37)	0.12 (0.15)	0.001** (0.1*)
T_a (°C per decade)	0.19 (0.12)	0.12 (0.12)	0.23 (0.73)
T_d (°C per decade)	0.58 (0.47)	0.21 (0.22)	0.04** (0.02**)
VPD (hPa per decade)	−0.13 (−0.24)	0.17 (0.17)	0.29 (0.1*)
RH (% per decade)	1.4 (1.2)	0.79 (0.81)	0.052* (0.18)
R_s (Ly day^{-1} decade^{-1})	1.8 (−0.3)	3.5 (4.2)	0.53 (0.73)
u_2 (m s^{-1} decade^{-1})	−0.04 (−0.05)	0.016 (0.014)	0.01** (0.002**)
E_o (mm per decade)	−28 (−50)	16 (16)	0.058*(0.002**)
E_p (mm per decade)	−18 (−18)	23 (22)	0.41 (0.34)

*Test significant at the 10% level. **Test significant at the 5% level.

seen from Figures 8 and 9, it is very different from the estimated actual ET rate, not only in its mean (1983–2015) annual value (544 ± 69 mm/year versus 1438 ± 62 mm/year) but also in its tendencies. While actual (irrigation) ET rates increase in the first part of the 1983–2015 period at a statistically significant linear rate (Table 3) and then drop, reference ET does the opposite: First, it drops and then increases in the second part of the period (Figure 9). Note that the CIMIS E_o values were never used for the actual ET estimates. The possible explanation for the large difference between actual and reference ET rates may include (without aiming to be comprehensive): (a) The grass around the CIMIS stations is not well irrigated, just irrigated, or barely/sporadically irrigated; (b) the grass is not healthy and actively growing throughout the entire measurement period as reference ET implies; and (c) the CIMIS station measurements may be influenced by energy advection from the surrounding nonirrigated sites (if such exist), which thus boosts both the E_o and E_p values, and the latter therefore depress the CR-estimated actual ET rates. The relative contributions of factors (a) to (c) are hard to specify.

The 544 ± 69-mm mean annual (1983–2015) plot-scale ET rate of the 10 CIMIS stations is 176 mm larger than the regional-scale irrigation ET rate of 368 ± 55 mm for the same period. Certainly, at the regional scale not all areas designated as irrigated by MIrAD are (a) actually irrigated over the whole study period as MIrAD is just a snapshot in time, (b) many are only periodically irrigated (e.g., during the growing season, the length of which may differ by crop/fruit type), and (c) the irrigated land percentage of the ~4-km PRISM cell may differ from the 1-km MIrAD cell designation due to the spatial aggregation of the latter values.

Overall, the tendencies found in the CIMIS plot-scale and the regional-scale irrigation ET values are similar: Estimated irrigation ET rates in general increase up to about 2,000 over the 1981–2007/1983–2007 periods (the latter period employed by Sorooshian et al., 2014) and then start to decline. The increasing irrigation ET tendencies are supported by similar increases in the dew point temperature (T_d) value, which via the $e_a = e_s(T_d)$ relationship is a measure of air humidity, that is, air humidity (and with it, RH) over irrigated fields increased in general in the 1983–2007/1981–2007 periods, both locally—at a statistically significant rate (Figure 9 and Table 3)—and regionally (Figure 7 and Table 2), providing a strong indication of rising irrigation ET rates in the same periods, as the CR estimates indeed predict. The CIMIS-measured air, dew point temperature, solar radiation, and precipitation rate tendencies either contradict the MM5-derived trends in Figure 4 of Sorooshian et al. (2014) or the July–August values they display are not representative of the whole year. The first possibility then may raise questions about the applicability of the MM5 reanalysis data, at least in the Central Valley of California. The PRISM T_a, T_d, and precipitation (and NARR u_2) tendencies, however, are all supported by the CIMIS data.

The dropping MM5-derived R_s, T_a, and air humidity values combined with similarly declining CIMIS E_o values may have led Sorooshian et al. (2014) to the conclusion that irrigation ET rates in the Central Valley declined overall in the 1981–2007 period. In fact, guided by the dropping CIMIS E_o values (Figure 9) in 1983–2007 and plot-scale soil moisture measurements at two locations they made changes in the soil moisture accounting algorithm of MM5 to boost its simulated ET values. This however raises the question of scale: How a regional-scale model ought to be best calibrated with plot-scale data? The answer to this question is beyond the scope of this study.

Important however is the realization that the CIMIS stations with their irrigated lawn environment do not evaporate at the potential rate, estimated by E_o. The E_o values yield a potential ET rate (E_p), that is, when soil moisture is not limiting. To see that the E_o values indeed behave as E_p values (e.g., those provided by ((2))), they were compared to the E_p values of WREVAP (Figure 10). The reason that the WREVAP E_p values are used for the comparison and not the ones provided by ((2)) is that the latter requires R_n, while WREVAP accepts the CIMIS measured R_s values as radiation input and estimates its own R_n values from that. Szilagyi and Jozsa (2008) demonstrated that the WREVAP E_p values are close to the ones ((2)) provides. Even though the WREVAP E_p values are larger than the E_o values of CIMIS, they behave similarly as the 0.84 value of the

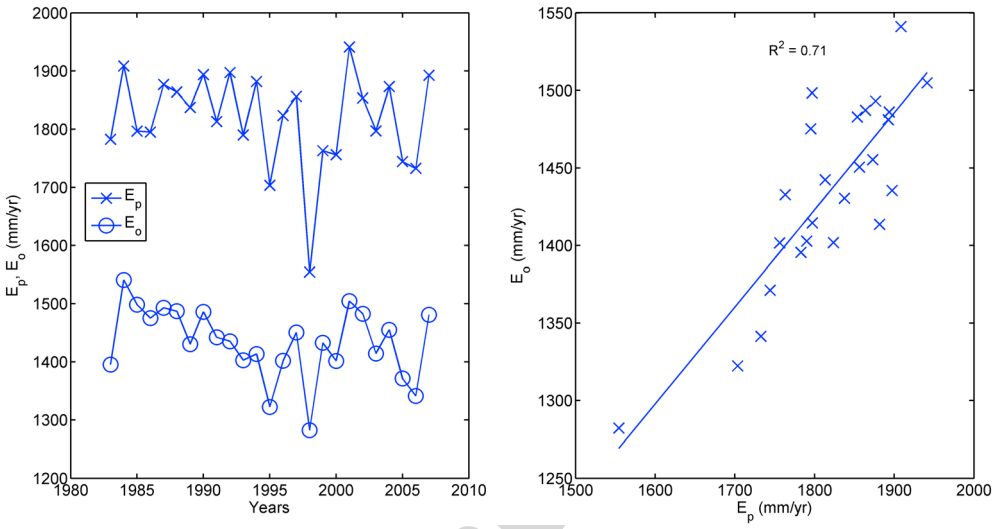

Figure 10. Annual California Irrigation Management Information System E_o (from monthly values of 10 stations) and WREVAP E_p values (1983–2007) and their scatter plot with the best linear fit ($E_o = 0.63E_p + 296$) displayed. The linear correlation coefficient (R) is 0.84.

linear correlation coefficient (R) indicates. The difference in evaporation rates may largely be explained by the differing bulk surface/aerodynamic resistances the two methods employ.

Acceptance of the E_o values as potential ET rate values (in fact, even CIMIS applies a variant of the Penman equation ((2)) of E_p and the Penman-Monteith equation of Allen et al., 1998, of E_o interchangeably) is an important step because then the CR helps explain why E_o must behave in a complementary way to actual irrigation ET. E_o kept dropping during 1983–2007 because actual irrigation ET rates (both plot scale and regional scale) were growing, testified independently by the CIMIS- and PRISM-measured increasing tendencies in the (irrigation) T_d, and RH values in 1983–2007 and 1981–2007, respectively. In the plot-scale CIMIS data the T_d increase was stronger than the one in T_a (Figure 9 and Table 3), leading to decreasing VPD values, which, when combined with a similarly decreasing u_2 value, will yield decreasing E_p and thus E_o rates, as can be seen from the terms in ((2)). The tendency of CIMIS R_n cannot directly be inferred from the CIMIS R_s tendency. WREVAP also estimated an E_p rate drop (due mostly to dropping VPD values) of about −18 (±23) millimeters per decade during 1983–2007 (Table 3) despite of not using wind data and an increase in estimated R_n (at a rate of about 11–16 [±10] millimeters per decade). For the regional-scale data the T_d rate increase was similar to the one in T_a (Figure 7 and Table 2) therefore VPD increased slightly even over irrigated fields but was counteracted by decreasing u_2 and R_n values leading to declining E_p rates (not shown) and thus to increasing regional-scale irrigation ET values in 1981–2007.

4. Summary and Conclusions

ET rates in three watersheds covering the Central Valley of California were modeled in the 1979–2015 time period, employing the CR of evaporation. The CR utilizes the inherent feedback mechanism between the soil moisture status and air humidity and derives actual ET rates complementary to potential evaporation ones. By doing so it avoids the application of conceptual models employed by land surface and, thus, by climate models typically requiring information of precipitation, vegetation cover, land use, physical soil type, thickness, field capacity, and hydraulic conductivity (among possible other soil/vegetation properties such as leaf area index and rooting depth), all spatially highly variable properties. Rather, the CR requires only basic atmospheric/radiation variables, such as air and dew point temperature, surface wind velocity, and net radiation.

With the help of the CR approach it was demonstrated that ET rates over the study area as a whole declined in both periods considered (similar to precipitation), that is, 1981–2007 and 1979–2015, at an overall linear rate of −6.3 ± 14 and −21 ± 6.8 mm per decade, respectively, the latter being statistically significant at the 5%

level. The ET rate decline was much stronger in the longer period because it included the mega-drought years of 2012–2015 at the end of the period.

The regional-scale ET trends for the two periods were validated with a water-balance approach that included the precipitation and area-averaged streamflow trend values and yielded a remarkable accuracy: The sum of the streamflow and CR-based ET trends was within 4% and 8% (i.e., for 1981–2007 and 1979–2015) of the observed precipitation trend values.

While watershed-scale ET rates declined in both periods, irrigation ET rates declined only in the 1979–2015 period at a linear rate of -16 ± 7.6 mm per decade (significant at the 10% level) and they increased during 1981–2007 at a meager rate of 2.6 ± 12 mm per decade, but this latter took place when precipitation over the same irrigated fields declined by -22 ± 30 mm per decade. In spite of the precipitation decline, dew point temperatures still rose during this period over the irrigated fields lending strong support for a corresponding irrigation ET rate increase. The irrigation ET rate increase of the 1981–2007 period contradicts earlier findings by Sorooshian et al. (2014) who employed a RCM (MM5) with NCEP reanalysis-I data and concluded that irrigation ET rates declined during the period. Because of these contrasting results, irrigation ET rates were further investigated with the help of the CIMIS plot-scale data.

CIMIS data corroborated the regional-scale findings: Irrigation ET rates derived from plot-scale data rose at a statistically significant linear rate of 31 ± 17 to 41 ± 17 mm per decade during 1983–2007, while at the same time CIMIS-measured precipitation dropped at a statistically significant linear rate of -36 ± 22 to -96 ± 31 mm per decade, indicating that for many years, irrigation could supplant the missing precipitation. Increasing irrigation ET rates at the plot-scale were also accompanied by a statistically significant linear increase in dew point temperature and RH. However, around the turn of the century, plot-scale irrigation ET rates also started to decline, similar to regional-scale irrigation ET values, causing both dew point temperature and RH values to drop.

The reason for the irrigation ET rate reversal around the turn of the century is not clear, and it is not the scope of the present study, but increasing irrigation ET rates before the turn of the century most probably resulted from increasing demand for irrigation water as precipitation declined overall and air temperatures rose (even if irrigation efficiency might have improved), which then may have increased the price of water, which then led farmers to eventually use less water (perhaps through further improved irrigation efficiency and/or letting fields to go fallow), reflected in the dropping irrigation ET rates after about the year 2000.

Since irrigation is such a lifeblood for the Californian farmer who thus sustains an agriculture with a global impact, it is important to know how irrigation at such a massive scale affects the regional hydrological cycle in which ET is a very important component. By understanding the latter, one can derive information on, for example, how droughts affect the water use in the Central Valley, which then can be applied in formulating different drought management response and prevention/early warning strategies.

It is hoped that the capability of the CR approach demonstrated here—especially in the light of recent developments (Brutsaert, 2015; Crago et al., 2016; Szilagyi, 2018b; Szilagyi et al., 2017) in CR research—in predicting regional-scale ET rates will attract the somewhat overdue attention of hydrometeorologists and especially climate modelers for improving the LSM components of the existing RCM/GCMs through their possible calibration and verification, employing the CR-based ET rates.

Acknowledgments

The CR-based monthly ET rates for 1979–2015 covering the coterminous United States can be requested from the corresponding author. The authors are grateful to J. Huntington and two other anonymous reviewers for their comments that lead to important revisions. All data used in this study are publicly available from the following sites: waterwatch.usgs.gov (runoff), www.prism.oregonstate.edu (PRISM), www.esrl.noaa.gov/psd/data/gridded/data.narr.html (NARR), http://ccar.colorado.edu/grace/jpl.html (GRACE), and http://www.cimis.water.ca.gov (CIMIS data).

References

Adoegoke, J., Pielke, R. Sr., Eastman, J., Mahmood, R., & Hubbard, K. (2003). Impact of irrigation on midsummer surface fluxes and temperature under dry synoptic conditions: A regional atmospheric model study of the U.S. High Plains. *Monthly Weather Review*, *131*(3), 556–564. https://doi.org/10.1175/1520-0493(2003)131<0556:IOIOMS>2.0.CO;2

Allen, R. G. (1996). Assessing integrity of weather data for use in reference evapotranspiration estimation. *Journal of Irrigation and Drainage Engineering, ASCE*, *122*(2), 97–106. https://doi.org/10.1061/(ASCE)0733-9437(1996)122:2(97)

Allen, R. G., Pereira, L. S., Raes, D., & Smith, M. (1998). Crop evapotranspiration: guidelines for computing crop water requirements. FAO irrigation and drainage paper 56, Food and Agriculture Organization of the United Nations, Rome, 300 p. Available at: http://www.fao.org/docrep/x0490e/x0490e00.htm

ASCE-EWRI (2005). The ASCE standardized reference evapotranspiration equation. Report 0–7844-0805-X, ASCE task committee on standardization of reference evapotranspiration, Reston, Virginia, American Society of Civil Engineers, available at https://goo.gl/JmjNfb

Berg, N., & Hall, A. (2015). Increased interannual precipitation extremes over California under climate change. *Journal of Climate*, *28*(16), 6324–6334. https://doi.org/10.1175/JCLI-D-14-00624.1

Bouchet, R. J. (1963). Evapotranspiration reelle, evapotranspiration potentielle, et production agricole. *Annales Agronomique*, *14*, 743–824.

Brown, J. F., & Pervez, M. S. (2014). Merging remote sensing data and national agricultural statistics to model change in irrigated agriculture. *Agricultural Systems*, *127*, 28–40. https://doi.org/10.1016/j.agsy.2014.01.004

Brutsaert, W. (1982). *Evaporation into the atmosphere: Theory, history and applications*. Dordrecht, Holland: D. Reider. https://doi.org/10.1007/978-94-017-1497-6

Brutsaert, W. (2015). A generalized complementary principle with physical constraints for land-surface evaporation. *Water Resources Research*, *51*, 8087–8093. https://doi.org/10.1002/2015WR017720

Brutsaert, W., & Stricker, H. (1979). An advection-aridity approach to estimate actual regional evapotranspiration. *Water Resources Research*, *15*(2), 443–450. https://doi.org/10.1029/WR015i002p00443

Christy, J. R., Norris, W. B., Redmond, K., & Gallo, K. P. (2006). Methodology and results of calculating central California surface temperature trends: Evidence of human-induced climate change? *Journal of Climate*, *19*(4), 548–563. https://doi.org/10.1175/JCLI3627.1

Crago, R., Szilagyi, J., Qualls, R. J., & Huntington, J. (2016). Rescaling of the complementary relationship for land surface evaporation. *Water Resources Research*, *52*, 8461–8471. https://doi.org/10.1002/2016WR019753

Daly, C., Halbleib, M., Smith, J. I., Gibson, W. P., Doggett, M. K., Taylor, G. H., et al. (2008). Physiographically sensitive mapping of climatological temperature and precipitation across the conterminous United States. *International Journal of Climatology*, *28*(15), 2031–2064. https://doi.org/10.1002/joc.1688

Daly, C., Neilson, R. P., & Phillip, D. L. (1994). A statistical topographic model for mapping climatological precipitation over mountainous terrain. *Journal of Applied Meteorology*, *33*(2), 140–158. https://doi.org/10.1175/1520-0450(1994)033<0140:ASTMFM>2.0.CO;2

de Vries, D. A. (1959). The influence of irrigation on the energy balance and the climate near the ground. *Journal of Meteorology*, *16*(3), 256–270. https://doi.org/10.1175/1520-0469(1959)016<0256:TIOIOT>2.0.CO;2

Diffenbaugh, N. S., Swaina, D. L., & Toumaa, D. (2015). Anthropogenic warming has increased drought risk in California. *Proceedings of the National Academy of Sciences U.S.A.*, *112*(13), 3931–3936. https://doi.org/10.1073/pnas.1422385112

Dyer, A. J., & Crawford, T. V. (1965). Observations of the modification of the microclimate at a leading edge. *Quarterly Journal of the Royal Meteorological Society*, *91*(389), 345–348. https://doi.org/10.1002/qj.49709138909

Guo, J. (2015). Agriculture is 80 percent of water use in California. Why aren't farmers being forced to cut back? *Washington Post*, April 3.

Hamed, K. H., & Rao, A. R. (1998). A modified Mann-Kendall trend test for autocorrelated data. *Journal of Hydrology*, *204*(1-4), 182–196. https://doi.org/10.1016/S0022-1694(97)00125-X

Hanak, E., Lund, J., Dinar, A., Gray, B., Howitt, R., Mount, J., et al. (2011). *Managing California's water: From conflict to reconciliation*, (p. 500). San Francisco, CA: Public Policy Institute of California.

Held, I. M., & Soden, B. J. (2006). Robust responses of the hydrological cycle to global warming. *Journal of Climate*, *19*(21), 5686–5699. https://doi.org/10.1175/JCLI3990.1

Hobbins, M. T., Ramirez, J. A., Brown, T. C., & Claessens, L. H. J. M. (2001). The complementary relationship in estimation of regional evapotranspiration: The complementary relationship areal evaporation and advection–aridity models. *Water Resources Research*, *37*(5), 1367–1387. https://doi.org/10.1029/2000WR900358

Huang, X., & Ullrich, P. A. (2016). Irrigation impacts on California's climate with the variable-resolution CESM. *Journal of Advances in Modeling Earth Systems*, *8*(3), 1151–1163. https://doi.org/10.1002/2016MS000656

Huntington, J. L., Gangopadhyay, S., Spears, M., Allen, R., King, D., Morton, C., et al. (2015). West-wide climate risk assessments: Irrigation demand and reservoir evaporation projections. U.S. Bureau of Reclamation, Technical memorandum No. 68-68210-2014-01, 196p., available at http://www.usbr.gov/watersmart/wcra/

Huntington, J. L., Hegewisch, K. C., Daudert, B., Morton, C. G., Abatzoglou, J. T., McEvoy, D. J., & Erickson, T. (2017). Climate Engine: Cloud computing and visualization of climate and remote sensing data for advanced natural resource monitoring and process understanding. *Bulletin of the American Meteorological Society*, *98*(11), 2397–2410. https://doi.org/10.1175/BAMS-D-15-00324.1

Huntington, J. L., Szilagyi, J., Tyler, S. W., & Pohll, G. M. (2011). Evaluating the complementary relationship for estimating evaporation from arid shrublands. *Water Resources Research*, *47*, W05533. https://doi.org/10.1029/2010WR009874

Jin, J., & Miller, N. L. (2011). Regional simulations to quantify land use change and irrigation impacts on hydroclimate in the California Central Valley. *Theoretical and Applied Climatology*, *104*(3-4), 429–442. https://doi.org/10.1007/s00704-010-0352-1

Kanamaru, H., & Kanamitsu, M. (2008). Model diagnosis of nighttime minimum temperature warming during summer due to irrigation in the California Central Valley. *Journal of Hydrometeorology*, *9*(5), 1061–1072. https://doi.org/10.1175/2008JHM967.1

Kueppers, L., & Snyder, M. (2012). Influence of irrigated agriculture on diurnal surface energy and water fluxes, surface climate, and atmospheric circulation in California. *Climate Dynamics*, *38*(5–6), 1017–1029. https://doi.org/10.1007/s00382-011-1123-0

Kueppers, L., et al. (2008). Seasonal temperature response to land-use change in the western United States. *Global and Planetary Change*, *60*(3-4), 250–264. https://doi.org/10.1016/j.gloplacha.2007.03.005

Kueppers, L. M., Snyder, M. A., & Sloan, L. C. (2007). Irrigation cooling effect: Regional climate forcing by land-use change. *Geophysical Research Letters*, *34*, L03703. https://doi.org/10.1029/2006GL 028679

Lo, M., & Famiglietti, J. S. (2013). Irrigation in California's Central Valley strengthens the southwestern U.S. water cycle. *Geophysical Research Letters*, *40*(2), 301–306. https://doi.org/10.1002/grl.50108

Lobell, D., Bala, G., Mrin, A., Phillips, T., Maxwell, R., & Rotman, D. (2009). Regional differences in the influence of irrigation on climate. *Journal of Climate*, *22*(8), 2248–2255. https://doi.org/10.1175/2008JCLI2703.1

Lobell, D. B., & Bonfils, C. (2008). The effect of irrigation on regional temperatures: A spatial and temporal analysis of trends in California, 1934–2002. *Journal of Climate*, *21*(10), 2063–2071. https://doi.org/10.1175/2007JCLI1755.1

Mahmood, R., Pielke, R. A. Sr., Hubbard, K. G., Niyogi, D., Bonan, G., Lawrence, P., et al. (2010). Impact of land use/land cover change on climate and future research priorities. *Bulletin of the American Meteorological Society*, *91*(1), 37–46. https://doi.org/10.1175/2009BAMS2769.1

McMahon, T. A., Peel, M. C., Lowe, L., Srikanthan, R., & McVicar, T. R. (2013a). Estimating actual, potential, reference crop and pan evaporation using standard meteorological data: A pragmatic synthesis. *Hydrology and Earth System Sciences*, *17*(4), 1331–1363. https://doi.org/10.5194/hess-17-1331-2013

McMahon, T. A., Peel, M. C., & Szilagyi, J. (2013b). Comment on the application of the Szilagyi–Jozsa advection–aridity model for estimating actual terrestrial evapotranspiration in "Estimating actual, potential, reference crop and pan evaporation using standard meteorological data: A pragmatic synthesis" by McMahon et al. (2013). *Hydrology and Earth System Sciences*, *17*(12), 4865–4867. https://doi.org/10.5194/hess-17-4865-2013

Mesinger, F., DiMego, G., Kalnay, E., Mitchell, K., Shafran, P. C., Ebisuzaki, W., et al. (2006). North American Regional Reanalysis. *Bulletin of the American Meteorological Society*, *87*(3), 343–360. https://doi.org/10.1175/BAMS-87-3-343

Monteith, J. L. (1981). Evaporation and surface temperature. *Quarterly Journal of the Royal Meteorological Society*, *107*(451), 1–27. https://doi.org/10.1002/qj.49710745102

Morton, F. I. (1983). Operational estimates of areal evapotranspiration and their significance to the science and practice of hydrology. *Journal of Hydrology*, *66*(1-4), 1–76. https://doi.org/10.1016/0022-1694(83)90177-4

Morton, F.I., Ricard, F., & Fogarasi, F. (1985). Operational estimates of areal evapotranspiration and lake evaporation—Program WREVAP. National Hydrologic Research Institute Paper No. 24. Ottawa, Canada.

Mount, J., & Hanak, E. (2016). Water use in California, Public Policy Institute of California. http://www.ppic.org/publication/water-use-in-california/, last accessed June 11, 2018.

Nau, R. F. (2017). Notes on regression and time series analysis. http://people.duke.edu/~rnau/forecasting.htm, last accessed January 28, 2018.

Ozdogan, M., Rodell, M., Beaudoing, H., & Toll, D. (2010). Simulating the effect of irrigation over the United States in a land surface model based on satellite-derived agricultural data. *Journal of Hydrometeorology*, *11*(1), 171–184. https://doi.org/10.1175/2009JHM1116.1

Penman, H. L. (1948). Natural evaporation from open water, bare soil, and grass. *Proceedings of the Royal Society of London*, *A193*, 120–146.

Pielke, R. A. Sr., Pitman, A., Niyogi, D., Mahmood, R., McAlpine, C., Hossain, F., et al. (2011). Land use/land cover changes and climate: Modeling analysis and observational evidence. *WIREs Climate Change*, *2*(6), 828–850. https://doi.org/10.1002/wcc.144

Priestley, C. H. B., & Taylor, R. J. (1972). On the assessment of surface heat flux and evaporation using large-scale parameters. *Monthly Weather Review*, *100*(2), 81–92. https://doi.org/10.1175/1520-0493(1972)100<0081:OTAOSH>2.3.CO;2

Rao, K. S., Wyngaard, J. C., & Cote, O. R. (1974). Local advection of momentum, heat, and moisture in micrometeorology. *Boundary-Layer Meteorology*, *7*(3), 331–348. https://doi.org/10.1007/BF00240836

Rider, N. E., Philip, J. R., & Bradley, E. F. (1963). The horizontal transport of heat and moisture—A micrometeorological study. *Quarterly Journal of the Royal Meteorological Society*, *89*(382), 507–531. https://doi.org/10.1002/qj.49708938207

Sacks, W., Cook, B., Buenning, N., Kevis, S., & Helkowski, J. (2009). Effects of global irrigation on the near-surface climate. *Climate Dynamics*, *33*(2-3), 159–175. https://doi.org/10.1007/s00382-008-0445-z

Seaber, P. R., Kapinos, F. P., & Knapp, G. L. (1987). Hydrologic unit maps. USGS water supply paper 2294.

Sorooshian, S., AghaKouchak, A., & Li, J. (2014). Influence of irrigation on land hydrological processes over California. *Journal of Geophysical Research: Atmospheres*, *119*, 13,137–13,152. https://doi.org/10.1002/2014JD022232

Sorooshian, S., Li, J., Hsu, K., & Gao, X. (2011). How significant is the impact of irrigation on the local hydroclimate in California's Central Valley? Comparison of model results with ground and remote-sensing data. *Journal of Geophysical Research*, *116*, D06102. https://doi.org/10.1029/2010JD01775

Sorooshian, S., Li, J., Hsu, K., & Gao, X. (2012). Influence of irrigation schemes used in RCMs on ET estimation: Results and comparative studies from California's Central Valley agricultural regions. *Journal of Geophysical Research*, *117*, D06107. https://doi.org/10.1029/2011JD016978

State of California (2013). California water plan, update 2013. Volume 1—The strategic plan.

Szilagyi, J. (2007). On the inherent asymmetric nature of the complementary relationship of evaporation. *Geophysical Research Letters*, *34*, L02405. https://doi.org/10.1029/2006GL028708

Szilagyi, J. (2014). Temperature corrections in the Priestley-Taylor equation of evaporation. *Journal of Hydrology*, *519*, 455–464. https://doi.org/10.1016/j.jhydrol.2014.07.040

Szilagyi, J. (2015). Complementary-relationship-based 30 year normals (1981–2010) of monthly latent heat fluxes across the contiguous United States. *Water Resources Research*, *51*, 9367–9377. https://doi.org/10.1002/2015WR017693

Szilagyi, J. (2018a). Anthropogenic hydrological cycle disturbance at a regional scale: State-wide evapotranspiration trends (1979-2015) across Nebraska, USA. *Journal of Hydrology*, *557*, 600–612. https://doi.org/10.1016/j.jhydrol.2017.12.062

Szilagyi, J. (2018b). A calibration-free, robust estimation of monthly land surface evapo-transpiration rates for continental-scale hydrology. *Hydrology Research*, *49*(3), 648–657. https://doi.org/10.2166/nh.2017.078

Szilagyi, J., Crago, R., & Qualls, R. J. (2017). A calibration-free formulation of the complementary relationship of evaporation for continental-scale hydrology. *Journal of Geophysical Research: Atmospheres*, *122*, 264–278. https://doi.org/10.1002/2016JD025611

Szilagyi, J., & Jozsa, J. (2008). New findings about the complementary relationship based evaporation estimation methods. *Journal of Hydrology*, *354*(1-4), 171–186. https://doi.org/10.1016/j.jhydrol.2008.03.008

Szilagyi, J., & Jozsa, J. (2009). Analytical solution of the coupled 2-D turbulent heat and vapor transport equations and the complementary relationship of evaporation. *Journal of Hydrology*, *372*(1-4), 61–67. https://doi.org/10.1016/j.jhydrol.2009.03.035

Wei, J., Dirmeyer, P. A., Wisser, D., Bosilovich, M. G., & Mocko, D. M. (2013). Where does the irrigation water go? An estimate of the contribution of irrigation to precipitation using MERRA. *Journal of Hydrometeorology*, *14*(1), 275–289. https://doi.org/10.1175/JHM-D-12-079.1

Yang, Z., Dominguez, F., Zeng, X., Hu, H., Gupta, H., & Yang, B. (2017). Impact of irrigation over the California Central Valley on regional climate. *Journal of Hydrometeorology*, *18*(5), 1341–1357. https://doi.org/10.1175/JHM-D-16-0158.1

Yoon, J.-H., Wang, S. S., Gillies, R. R., Kravitz, B., Hipps, L., & Rasch, P. J. (2015). Increasing water cycle extremes in California and relation to ENSO cycle under global warming. *Nature Communications*, *6*(1), 8657. https://doi.org/10.1038/ncomms9657